# Application of Hierarchical Cascading Technique to FEM Simulation in BAW Devices

階層的縦続法の BAW デバイスの有限要素シミュレーションへの適用

Xinyi Li[1,2‡], Jingfu Bao[1], Yulin Huang[1,2], Benfeng Zhang[3,2], Tatsuya Omori[2] and Ken-ya Hashimoto[2,3]
([1]Univ. Elect. Sci. Technol. China; [2]Chiba Univ.; [3]Shanghai Jiao Tong Univ.)
李昕熠 [1,2‡],鮑景富 [1],黄裕霖 [1,2],張本鋒 [3,2],大森達也 [2],橋本研也 [2,3] ([1] 電子科技大, [2] 千葉大, [3] 上海交通大)

## 1. Introduction

Finite element method (FEM) simulation[1] is widely used in designing ultrasonic devices, such as SAW/BAW resonators[2,3]. In many cases, FEM models are composed of a large number of degrees-of-freedom (DOFs), and required computer power and memory size are enormous.

In 2016, Koskela, et al. proposed hierarchical cascading approach for FEM simulation of SAW devices[4]. It is based on elimination of inner DOFs from a unit block and its cascading. Thus provided that the model under concern is composed of periodic elements, required memory size can be reduced drastically, and the FEM simulation can be performed very quickly.

The authors proposed use of traveling wave excitation sources (TWESs) for the FEM analysis of SAW/BAW scattering[5]. It was shown that this technique is quite effective for the scattering analysis at the side border of BAW devices and that at the aperture edges of SAW devices.

This paper describes use of the hierarchical cascading approach for the TWESs based FEM analysis of BAW devices. An efficient absorbing mechanism is developed to replace the perfectly matched layer (PML). The calculated results and calculation time are compared with those of the original whole FEM analysis.

## 2. Hierarchical cascading FEM matrix

The basic theory of hierarchical cascading FEM matrices is given in [4]. Here we summarize the hierarchical cascading approach modified for this work.

First, the whole FEM model is divided into some different units for SAW/BAW simulation,. The FEM matrix of each unit is expressed as:

$$\begin{pmatrix} \boldsymbol{A}_{11} & \boldsymbol{A}_{12} & \boldsymbol{0} \\ \boldsymbol{A}_{21} & \boldsymbol{A}_{22} & \boldsymbol{A}_{23} \\ \boldsymbol{0} & \boldsymbol{A}_{32} & \boldsymbol{A}_{33} \end{pmatrix} \begin{pmatrix} \boldsymbol{x}_{\mathrm{L}} \\ \boldsymbol{x}_{\mathrm{I}} \\ \boldsymbol{x}_{\mathrm{R}} \end{pmatrix} = \begin{pmatrix} \boldsymbol{L}_{\mathrm{L}} \\ \boldsymbol{L}_{\mathrm{I}} \\ \boldsymbol{L}_{\mathrm{R}} \end{pmatrix}, \qquad (1)$$

where $\boldsymbol{A}_{ij}$ are sub-matrices, $\boldsymbol{x}$ and $\boldsymbol{L}$ are DOFs and surface forces, and subscripts R, L, and I indicate values at left/right boundaries and in interior, respectively. Elimination of $\boldsymbol{x}_{\mathrm{I}}$ from Eq. (1) gives

$$\begin{pmatrix} \boldsymbol{B}_{11} & \boldsymbol{B}_{12} \\ \boldsymbol{B}_{21} & \boldsymbol{B}_{22} \end{pmatrix} \begin{pmatrix} \boldsymbol{x}_{\mathrm{L}} \\ \boldsymbol{x}_{\mathrm{R}} \end{pmatrix} = \begin{pmatrix} \boldsymbol{L}_{\mathrm{L}} - \boldsymbol{A}_{12}\boldsymbol{A}_{22}^{-1}\boldsymbol{L}_{\mathrm{I}} \\ \boldsymbol{L}_{\mathrm{R}} - \boldsymbol{A}_{32}\boldsymbol{A}_{22}^{-1}\boldsymbol{L}_{\mathrm{I}} \end{pmatrix}. \qquad (2)$$

where

$$\begin{pmatrix} \boldsymbol{B}_{11} & \boldsymbol{B}_{12} \\ \boldsymbol{B}_{21} & \boldsymbol{B}_{22} \end{pmatrix} = \begin{pmatrix} \boldsymbol{A}_{11} - \boldsymbol{A}_{12}\boldsymbol{A}_{22}^{-1}\boldsymbol{A}_{21} & -\boldsymbol{A}_{12}\boldsymbol{A}_{22}^{-1}\boldsymbol{A}_{23} \\ -\boldsymbol{A}_{32}\boldsymbol{A}_{22}^{-1}\boldsymbol{A}_{21} & \boldsymbol{A}_{33} - \boldsymbol{A}_{32}\boldsymbol{A}_{22}^{-1}\boldsymbol{A}_{23} \end{pmatrix}. \qquad (3)$$

Note that $\boldsymbol{x}_{\mathrm{I}}$ is related to $\boldsymbol{x}_{\mathrm{L}}$ and $\boldsymbol{x}_{\mathrm{R}}$ as

$$\boldsymbol{x}_{\mathrm{I}} = \boldsymbol{A}_{22}^{-1}\left(\boldsymbol{L}_{\mathrm{I}} - \boldsymbol{A}_{21}\boldsymbol{x}_{\mathrm{L}} - \boldsymbol{A}_{23}\boldsymbol{x}_{\mathrm{R}}\right). \qquad (4)$$

Next, let us consider two blocks labelled A and B are cascaded. Since $\boldsymbol{x}_{\mathrm{R}}^{\mathrm{A}}=\boldsymbol{x}_{\mathrm{L}}^{\mathrm{B}}$ and $\boldsymbol{L}_{\mathrm{R}}^{\mathrm{A}}+\boldsymbol{L}_{\mathrm{L}}^{\mathrm{B}}=0$, one may obtain the following equation with the same form as Eq. (1):

$$\begin{pmatrix} \boldsymbol{B}_{11}^{\mathrm{A}} & \boldsymbol{B}_{12}^{\mathrm{A}} & \boldsymbol{0} \\ \boldsymbol{B}_{21}^{\mathrm{A}} & \boldsymbol{B}_{22}^{\mathrm{A}} + \boldsymbol{B}_{11}^{\mathrm{B}} & \boldsymbol{B}_{12}^{\mathrm{B}} \\ \boldsymbol{0} & \boldsymbol{B}_{21}^{\mathrm{B}} & \boldsymbol{B}_{22}^{\mathrm{B}} \end{pmatrix} \begin{pmatrix} \boldsymbol{x}_{\mathrm{L}}^{\mathrm{A}} \\ \boldsymbol{x}_{\mathrm{R}}^{\mathrm{A}}(=\boldsymbol{x}_{\mathrm{L}}^{\mathrm{B}}) \\ \boldsymbol{x}_{\mathrm{R}}^{\mathrm{B}} \end{pmatrix} = \begin{pmatrix} \boldsymbol{L}_{\mathrm{L}}^{'} \\ \boldsymbol{L}_{\mathrm{I}}^{'} \\ \boldsymbol{L}_{\mathrm{R}}^{'} \end{pmatrix}. \qquad (5)$$

where $\boldsymbol{L}_{\mathrm{L}}^{'} = \boldsymbol{L}_{\mathrm{L}}^{\mathrm{A}} - \boldsymbol{A}_{12}^{\mathrm{A}}\boldsymbol{A}_{22}^{\mathrm{A\text{-}1}}\boldsymbol{L}_{\mathrm{I}}^{\mathrm{A}}$ , $\boldsymbol{L}_{\mathrm{R}}^{'} = \boldsymbol{L}_{\mathrm{R}}^{\mathrm{B}} - \boldsymbol{A}_{32}^{\mathrm{B}}\boldsymbol{A}_{22}^{\mathrm{B\text{-}1}}\boldsymbol{L}_{\mathrm{I}}^{\mathrm{B}}$ and $\boldsymbol{L}_{\mathrm{I}}^{'} = -\boldsymbol{A}_{32}^{\mathrm{A}}\boldsymbol{A}_{22}^{\mathrm{A\text{-}1}}\boldsymbol{L}_{\mathrm{I}}^{\mathrm{A}} - \boldsymbol{A}_{12}^{\mathrm{B}}\boldsymbol{A}_{22}^{\mathrm{B\text{-}1}}\boldsymbol{L}_{\mathrm{I}}^{\mathrm{B}}$. Thus total $\boldsymbol{B}$ matrix for the whole simulation model can be calculated by successive application of this algorithm (see **Fig.1**) .

All DOFs at boundaries can be calculated by giving appropriate boundary conditions to the side ends. Once boundary DOFs are obtained, inner DOFs can be also calculated using Eq.(4).

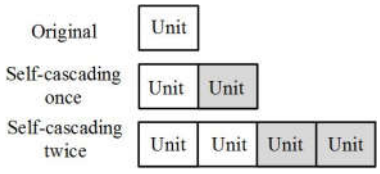


Fig.1 Hierarchical cascading algorithm

Due to iterative use of the identical working space, required memory size can be reduced significantly. Furthermore, in cases when many identical units are aligned, we can accelerate the calculation speed exponentially by recursive use of calculated $\boldsymbol{B}$ matrices at the hierarchical cascading[4].

## 3. Hierarchical Cascading TWES BAW model

The technique described above is applied in TWES BAW model shown in Fig.2. The

‡kimilee56@gmail.com

Ru/AlN/Ru composed mebrane is considered, and the setup is the same as that used in [5]. The frequency is set just below the cutoff frequency of the main (S1-) mode. Phase variation of TWES is set so that S1- Lamb mode with the wavenumber $\beta$ is predominantly excited at the active area and incident to the border area, and scattered waves are sensed at the passive area 2. These waves are finally absorbed at the damping area.

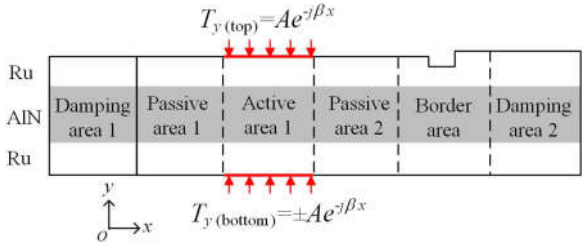


Fig. 2 Schematic TWES BAW model

The $\boldsymbol{B}$ matrix of the damping area was realized as follows: An isotropic loss factor is introduced to each unit, and the value gradually increases for a few units (models a-c), and is constant (model d) as shown in **Fig. 3.** The hierarchical cascading enables rapid calculation of the total $\boldsymbol{B}$ matrix of cascaded model-d's even when the number of region-d's is extremely large provided that the number is $n$-th power of 2. Since $\boldsymbol{x}_{\mathrm{L}}$ is regarded as zero when $n$ is sufficiently large, Eq. (2) can be simplified as $\boldsymbol{B}_{22}\boldsymbol{x}_{\mathrm{R}} = \boldsymbol{L}_{\mathrm{R}}$ for the damping area.

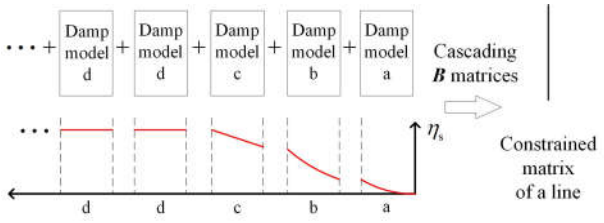


Fig. 3 Variation of loss factor in damping region where waves are incident from the right end.

The $\boldsymbol{B}$ matrix of the active area is also assembled by the hierarchical cascading including the phase shift in $\boldsymbol{L}$. To save time, passive areas shares the same $\boldsymbol{B}$ matrix with the active area but $\boldsymbol{L}$=**0**.

## 4. Simulation result

The following FEM modeling and simulation is realized by commercial software COMSOL. Post matrix operation is implemented in MATLAB via LiveLink from COMSOL.

The solved $\boldsymbol{B}$ matrix of the whole model is obtained after 11 times cascading operations excluding cascading for the damping areas (method 1). We also directly modeled and solved the whole model in COMSOL (method 2) for comparison. Because it is impossible to setup an infinite-length damping region in method 2. The damping area is shortened with a higher loss factor, which would somewhat worse the absorption effect. Two simulations were performed using the identical PC (CPU i7-5820K, 3.3 GHz, 128 GB RAM).

**Fig.4** shows the calculated amplitudes of out-of-plane vibration at the top surface in the passive area 2. Any differences are hardly seen between two results. Even it exists, it is hard to judge which method is more correct.

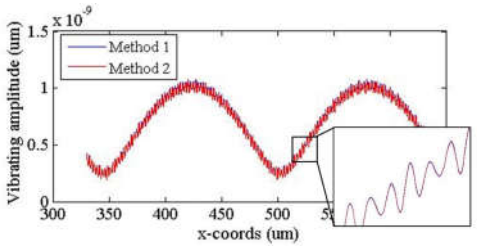


Fig.4 Calculated out-of-plane displacement

**Table I** shows amplitudes of reflected Lamb waves normalized by that of the incident S1- mode. The differences are very tiny (0.2 dB maximum)

Table I. Amplitude of reflected Lamb modes

| (dB) | S1- | S1+ | S0 | A1 | A0 |
|---|---|---|---|---|---|
| Method 1 | -3.81 | -36.64 | -23.47 | -42.6 | -35.9 |
| Method 2 | -3.83 | -36.58 | -23.47 | -42.4 | -36.0 |

For each frequency point, 0.9 and 15 seconds were spent for methods 1 and 2, respectively. It is worth to notice that the time consumption for the damping areas is not included in this calculation. Net difference of the calculation time is much larger.

It proves that the hierarchical cascading method is quite effective for the analysis of BAW devices using TWESs.

**Acknowledgment**

The work was partially supported by Grants-in-Aid for Scientific Research <KAKENHI> of Japan Society for the Promotion of Science. Xinyi Li acknowledges the support of the Japanese Government (MEXT) for the scholarship through the Super Global University Project.

**References**

[1] R.Courant: B. Am. Math. Soc., **49**, 1 (1943) p.1.
[2] M.Koshiba, et al., Jpn. J. Appl. Phys., **36**, 5S (1997) p.3060
[3] R.Thalhammer, et al., IEEE Trans. Ultrason. Ferroelec. & Freq. Contr., **63**, 10 (2016) p.1624
[4] J.Koskela, et al: *Proc. IEEE Ultrason. Symp.* (2016) p.122.
[5] X.Li, et al.: *Proc. IEEE Ultrason. Symp.* (2017) [to be published].